ADVANCED PHOTONICS RESEARCH
Open Access
www.adpr-journal.com

Biocompatible Polymer and Protein Microspheres with Inverse Photonic Glass Structure for Random Micro-Biolasers

Van Duong Ta, Soraya Caixeiro, Dhruv Saxena, and Riccardo Sapienza**

The miniaturization of random lasers to the micrometer scale is challenging but fundamental for the integration of lasers with photonic integrated circuits and biological tissues. Herein, it is demonstrated that random lasers with a diameter from 30 to 160 μm can be achieved by using a simple emulsion process and selective chemical etching. These tiny random laser sources are made of either dye-doped polyvinyl alcohol (PVA) or bovine serum albumin (BSA) and they are in the form of microporous spheres with monodisperse pores of 1.28 μm in diameter. Clear lasing action is observed when the microporous spheres are optically excited with powers larger than the lasing threshold, which is 154 μJ mm^{-2} for a 75 μm diameter PVA microporous sphere. The lasing wavelength redshifts 10 nm when the PVA microsphere diameter increases from 34 to 160 μm. For BSA microspheres, the lasing threshold is around 55 μJ mm^{-2} for a 70 μm diameter sphere and 104 μJ mm^{-2} for a 35 μm diameter sphere. The simple fabrication process reported allows for detail studies of morphology and size, important for fundamental studies of light–matter interaction in complex media, and applications in photonic integrated circuits, photonic barcoding, and optical biosensing.

1. Introduction

Random lasers have attracted a great deal of interest due to their rich physical properties and promising applications such as cost-effective light sources, photonic barcoding and speckle free bioimaging, and biosensing.[1] Random lasers are an unconventional source of stimulated emission which is provided by multiple scattering of light in disordered media.[2] As a result, random lasing is obtained via multiple scattering rather than resonant recirculation as in a conventional cavity. Various structures and materials have been used for random lasers such as fluorescent dye in colloidal suspensions,[3] quantum dots,[4,5] semiconductor powders,[6] self-assembled fluorescent nanoparticles,[7–10] nanowires,[11] and even dye-doped human tissue.[12]

Reducing the size of a random laser to microscale opens up many potential applications such as on-chip optical communications, data processing, and bio-integration.[13] To date, random microlasers are highly limited to semiconductor-based structure such as the clusters of ZnO nanoparticles,[14] and ZnO microwires[15] whereas organic random lasers generally have a larger size in a range of millimeter scale.[16–18] Compared with semiconductor random microlasers, organic random microlasers may have several advantages including low-cost fabrication, flexible properties, and lightweight.[19–21] However, obtaining small organic random microlasers is challenging as organic materials tend to have low refractive index and a highly disordered medium requires careful optimization.[20,22]

In this work, we demonstrate biocompatible organic random microlasers with diameters from 30 to 160 μm. An inverse photonic glass structure (spherical voids in a matrix)—a highly scattering medium[23] is manipulated to yield a microporous sphere. The fabrication technique can be applied to a variety of water-soluble polymers and proteins. Particularly, we demonstrate polyvinyl alcohol (PVA) and bovine serum albumin (BSA)-based random microlasers.

2. Fabrication of Microporous Spheres

Figure 1a–e describe the fabrication process of the microsphere random lasers by utilizing a simple emulsion and selective chemical etching. First, as shown in Figure 1a, a droplet of an aqueous mixture that contains a water-soluble polymer/protein and polystyrene (PS) microspheres is injected in a polydimethylsiloxane

Dr. V. D. Ta
Department of Optical Devices
Le Quy Don Technical University
Hanoi 100000, Vietnam
E-mail: duong.ta@lqdtu.edu.vn

Dr. S. Caixeiro
School of Physics and Astronomy
University of St Andrews
St Andrews KY16 9SS, UK

Dr. D. Saxena, Dr. R. Sapienza
The Blackett Laboratory
Department of Physics
Imperial College London
London SW7 2AZ, UK
E-mail: r.sapienza@imperial.ac.uk

The ORCID identification number(s) for the author(s) of this article can be found under https://doi.org/10.1002/adpr.202100036.

© 2021 The Authors. Advanced Photonics Research published by Wiley-VCH GmbH. This is an open access article under the terms of the Creative Commons Attribution License, which permits use, distribution and reproduction in any medium, provided the original work is properly cited.

DOI: 10.1002/adpr.202100036

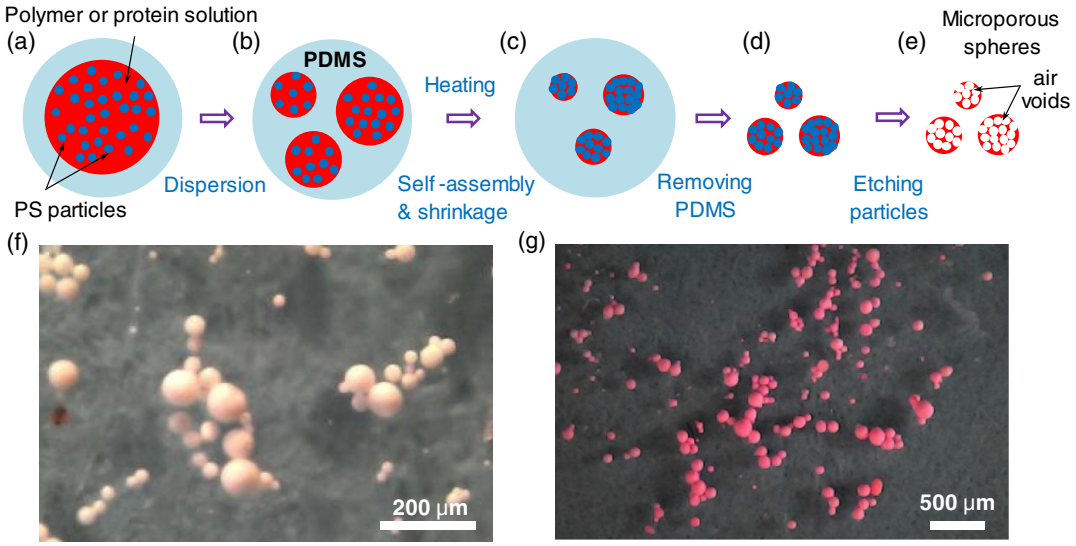

Figure 1. a–e) Schematic diagram describing the fabrication process of microporous spheres with inverse photonic glass structure. f,g) Optical images of microporous PVA spheres without doping dye (white color) and with doping RhB (red color), respectively.

(PDMS) base (Sylgard 184 Silicon Elastomer from Dow Corning). Subsequently, the droplet is dispersed by using a needle to create smaller droplets (Figure 1b). As water and PDMS are immiscible, these droplets are self-assembled due to surface tension. The droplets are then heated to evaporate all water leading to solid microspheres (Figure 1c). Next, the PDMS is dissolved in ethyl acetate, and solid spheres are obtained with a direct photonic glass structure, i.e., they are composed of PS microparticles in a polymer/protein matrix (Figure 1d). Finally, the refractive index contrast is improved by selectively etching the PS microparticles in ethyl acetate. The ethyl acetate solvent dissolves the PS particles but does not affect the polymer/protein host material. As a result, microporous polymer/protein spheres with an inverse photonic glass structure are obtained (Figure 1e). The microporous structure has a high refractive index contrast and consequently smaller transport mean free path which is a key property for low-threshold random lasing.[24]

Optical microscopy images of fabricated microporous spheres are shown in Figure 1f,g. PVA microporous spheres exhibit white color as expected because they scatter light strongly (Figure 1f). To turn these spheres into laser sources, organic dye Rhodamine B (RhB) molecules were added to the PVA initial solution thus dye-doped spheres demonstrate red color (Figure 1g). The microporous spheres are polydisperse with a diameter ranging from about 10 to 150 μm.

3. Microstructure and Lasing Properties of Microporous PVA Spheres

Using the aforementioned technique, microporous PVA spheres of different size were obtained. The host material PVA was chosen due to its high water solubility, biocompatibility, low-cost, and widely used in medical and dietary supplement products.[25] **Figure 2**a shows a scanning electron microscope (SEM) image of dye-doped microporous spheres with a diameter ranging from about 10 to 120 μm. High-magnification SEM images of two individual spheres with a diameter of 65 and 20 μm are shown in Figure 2b,c, exhibiting a spherical shape with a uniform microporous structure. As the PS microparticles are closely packed, the air voids are well connected and pores are expected to distribute uniformly all over the spheres. The air voids and PVA matrix are observed better in a close-up SEM image (Figure 2d).

Transport mean free path (l_t) is an important parameter for random lasers that characterizes the scattering strength and regime of light transport in the scattering medium.[24] l_t of a slab of random scattering material can be determined by the photonic Ohm's law.[26–28] For example, at visible wavelengths, l_t of a photonic glass made of 1.22 μm diameter PS spheres embedded in air is ≈3 μm [27] whereas l_t of natural coral skeletons is ≈20 μm.[28] In our work, measuring l_t of single microporous spheres is challenging because of their small size. However, it is possible to measure l_t for bulk geometries. l_t of a similar structure (the same pore size of 1.28 μm and packing density of ≈50%) was measured and it is around 4 μm for wavelength of 600 nm.[16,23]

One important parameter of the microspheres is porosity and it would affect the lasing threshold via the scattering parameters. We expect that the porosity of the dye-doped PVA spheres of different diameters would be similar, as these spheres were made by self-assembly from the same solution and in the same way. This is supported by SEM images of the dye-doped PVA microspheres of different diameters shown in Figure S1, Supporting Information.

Due to high scattering, dye-doped microporous spheres can act as excellent random microlasers under optical pumping. As shown in the inset of **Figure 3**a, the emission from the dye molecules is trapped and significantly enhanced by multiple scattering inside the microporous sphere before scattering outside in all directions. In Figure 3a, the evolution from fluorescent to lasing emission can be seen clearly from a 75 μm diameter

© 2021 The Authors. Advanced Photonics Research published by Wiley-VCH GmbH

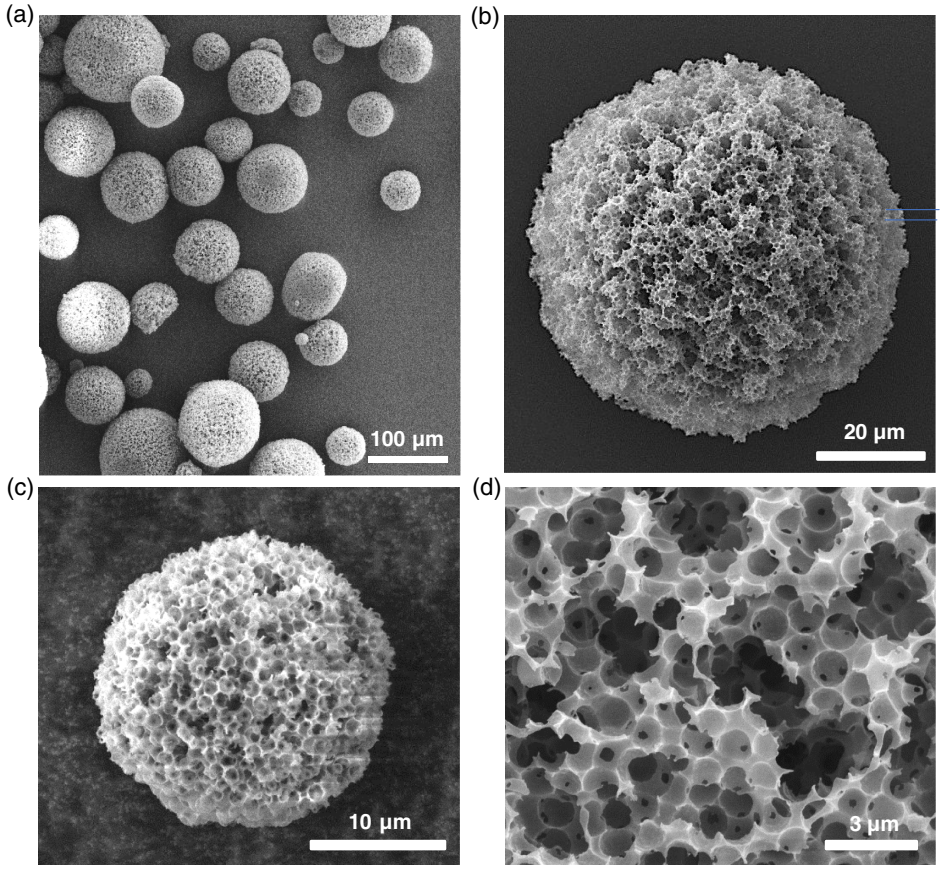

Figure 2. a) SEM image of fabricated microporous spheres with various diameters ranging from about 10 to 120 μm. b,c) SEM image of a single microporous sphere with a diameter of 65 and 20 μm, respectively. d) High-magnification SEM image of the microporous structure highlighting the air voids and the PVA structure.

sphere when increasing the pumping power above the lasing threshold of around 150 μJ mm^{-2}. For pumping fluence smaller than 116 μJ mm^{-2}, the sphere emits spontaneous emission that is characterized by low intensity and a broad spectrum. At 147 μJ mm^{-2}, the emission spectrum begins to narrow and the intensity increases sharply which is the evidence of stimulated emission. At 181 μJ mm^{-2}, the spectrum is very narrow with some spikes (linewidth of spikes is 0.2 nm, which is the spectral resolution of the spectrometer) and the intensity is very high, indicating the dominance of lasing emission. The photoluminescence (PL) image of the sphere shows bright emission (Figure 3b) and its brightness is much stronger when the pump energy is above the lasing threshold (Figure 3c).

We suggest that our random lasers working in the diffusive regime as the mean free path is much larger than the light wavelength, and thus, the chance for coherent feedback or loops/cavities inside is very low. As a result, the observation of some spikes in the lasing spectrum is quite interesting. Even though spikes and diffusion can coexist,[29] the reasons for spikes in lasing spectrum of diffusive random lasers are still not fully understood. This will be the subject of follow-up works.

To determine the lasing threshold value, PL peak intensity as a function of pump fluences is plotted in Figure 3d. The emitted intensity increases linearly with the pumping fluence until a sudden increase is observed at around 154 μJ mm^{-2} which we identify as the lasing threshold. The threshold energy is comparable to other polymeric random lasers based on photonic glass structure [8] and inverse opals.[18]

Another evidence of random lasing is spectral narrowing. Figure 3e indicates that the spectral linewidth of PL emission decreases with increasing pump fluence. At the lowest pump fluence (<21 μJ mm^{-2}), the spectral linewidth is very broad, around 47 nm. It decreases gradually and almost linearly to 5.5 nm at 181 μJ mm^{-2}. For higher pump fluences, the spectral linewidth reduces further (but with a lower rate) and reaches its minimum of 2.7 nm at 248 μJ mm^{-2}.

The size dependence of the lasing characteristics is investigated and it is found that the lasing spectrum and lasing wavelength fluctuate from sphere to sphere. As shown in **Figure 4**a, smaller microspheres exhibit narrower spectral linewidth and shorter lasing wavelength. One interpretation can be that smaller spheres have fewer lasing modes thus the overall spectral linewidth is narrower. The number of modes of 2D diffusive random lasers within the gain bandwidth depends on size of the system.[30] In any dimension, the number of modes in a volume is expected to be constant, on average, as is the density of optical states. However, it is hard to provide a specific theoretical model for the modes of random lasers in our system because our lasers

© 2021 The Authors. Advanced Photonics Research published by Wiley-VCH GmbH

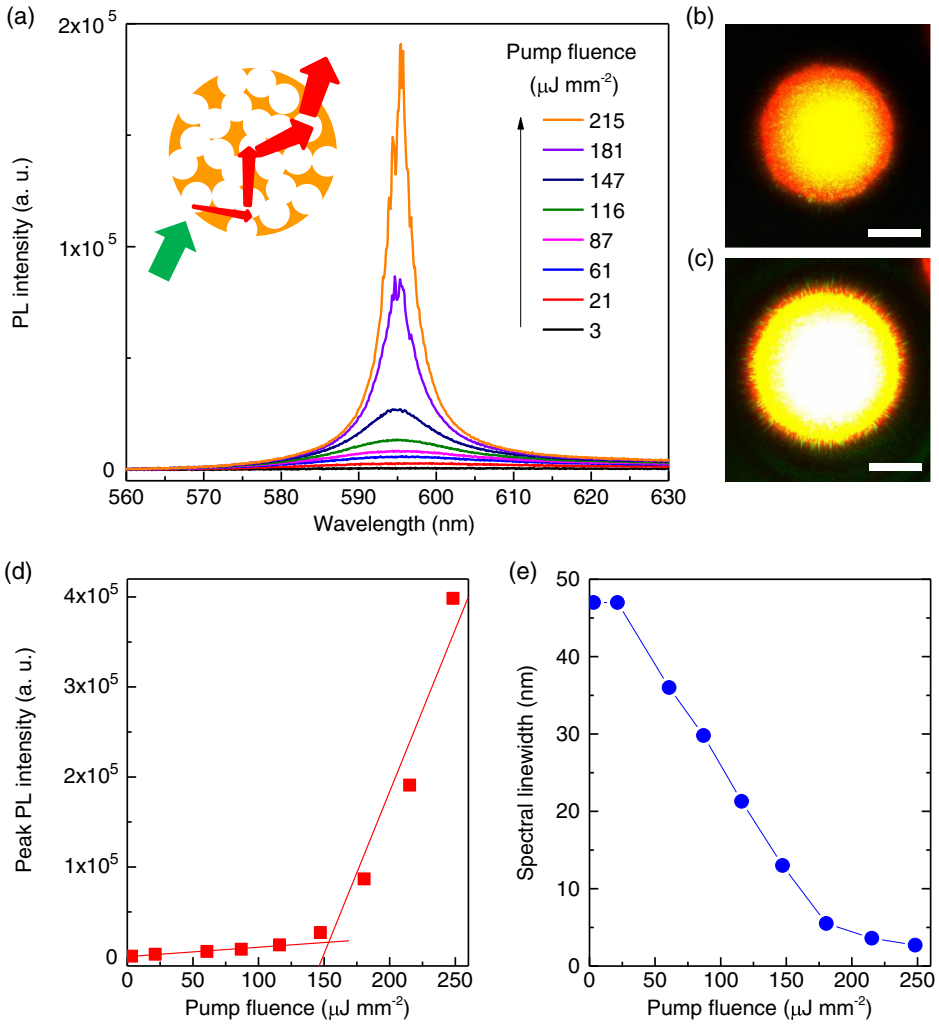

Figure 3. a) Emission spectra of a 75 μm diameter sphere under various pump pulse fluences. The inset indicates a schematic of light amplification via multiple scattering in a microporous sphere. b,c) PL microscope image of the sphere below and above the lasing threshold, respectively. The scale bars are 30 μm. d,e) PL peak intensity and spectral linewidth of the emission of the sphere as a function of pump fluence, respectively.

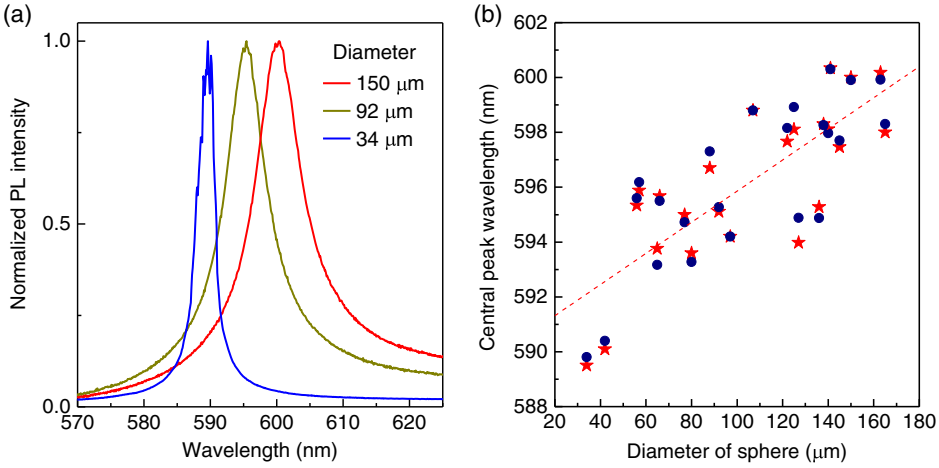

Figure 4. a) Normalized PL intensity of three different microporous spheres at the pump fluence of about 1.6 times higher than the lasing threshold of each sphere. b) Central peak wavelength versus diameter of microporous spheres above threshold (red stars) and below threshold (blue dots).

© 2021 The Authors. Advanced Photonics Research published by Wiley-VCH GmbH

are 3D microspheres. As a result, we plan to address this outstanding challenge and to develop the theoretical model in the future work.

Regarding the wavelength shift, light travels a longer path inside bigger spheres and thus has a greater chance of being reabsorbed by the dye molecules (absorption and emission spectra of RhB solution is shown in Figure S2, Supporting Information). Large spheres, with diameters above the scattering mean free path, are also less efficiently pumped because of scattering of the pump light, leading to larger unpumped regions that contribute to absorption. Since absorption is stronger at shorter wavelengths, the stronger absorption/reabsorption of light in larger spheres results in an effective redshift of the peak intensity. A more statistical investigation of the wavelength shift is shown in Figure 4b, indicating a redshift of around 10 nm when the sphere diameter increases from 40 to 160 μm. The redshift of the peak intensity is also apparent in the fluorescence spectrum (below threshold), which further supports that reabsorption is the reason for the observed redshift. This wavelength shift depends on sphere diameter thus it provides an opportunity for obtaining a desired lasing wavelength in a certain range. For example, if the sphere size can be controlled by using some advanced techniques such as inkjet printing or microfluidics,[31,32] the output lasing wavelength can be precisely tuned.

It is worth noting that the sphere had to be dried out to see lasing as this provides a high enough index contrast. So far, they can only lase in the air. However, if they were sealed, they can be used in an aqueous solution. This issue will be studied in the future works. In addition, these lasers are soft, lightweight, and can be deformed. Lasing emission can be tuned by mechanical deformation.[21]

4. Microstructure and Lasing Properties of Microporous BSA Spheres

Our unique fabrication technique can be applied to different water-soluble materials. Herein, we chose BSA as an alternative material for the host material due to its desirable biocompatibility, biodegradability properties,[33] and its good integration with organic dye molecules.[34,35] **Figure 5**a shows BSA with different size can be fabricated. A SEM image of a typical dye-doped BSA sphere exhibits a spherical shape with a diameter of about 63 μm (Figure 5b). It is quite porous and the surface porosity is presented in a higher magnification SEM (Figure 5c). The pores on the surface of the BSA sphere have a different morphology when compared with the PVA microspheres which may be due to the alteration of protein structure and subsequent swelling caused by the heating process. In some case, the pores are not visible, however, as shown in Figure 5d and Figure S3, Supporting Information, for broken spheres, the pores are present. Due to the difference in chemical and physical properties, the porosity of the BSA structure is generally different from the PVA structure.

Similar to PVA spheres, BSA spheres emit random lasing under optical pumping. **Figure 6**a,b show the evolution from spontaneous to lasing emission of a 35 μm diameter and a 70 μm diameter sphere, respectively. It is found that the smaller laser needs higher pump energy to reach the lasing emission. Particularly, the lasing threshold of the 35 μm diameter is 104 μJ mm^{-2} which is about two times higher compared with 51 μJ mm^{-2} of the 70 μm diameter sphere (Figure 6c).

The size dependence of the lasing threshold can be explained. For a random laser, the lasing threshold depends on many factors including the transport mean free path, the gain, and size. Herein, the transport mean free path and the gain are expected to be similar between BSA spheres, the only factor that affects the lasing threshold is the sphere's size. In a larger sphere, the light emission can travel a longer path consequently leading to easier amplification. As a result, the larger sphere would have a lower lasing threshold compared with the smaller one. The result is consistent with previous studies where the lasing threshold of a ZnO film[36] or direct photonic glass structure would decrease with increasing pumping spot.[8]

It is noted that the lasing spectrum (linewidth and peak) looks very similar between PVA and BSA porous spheres of similar

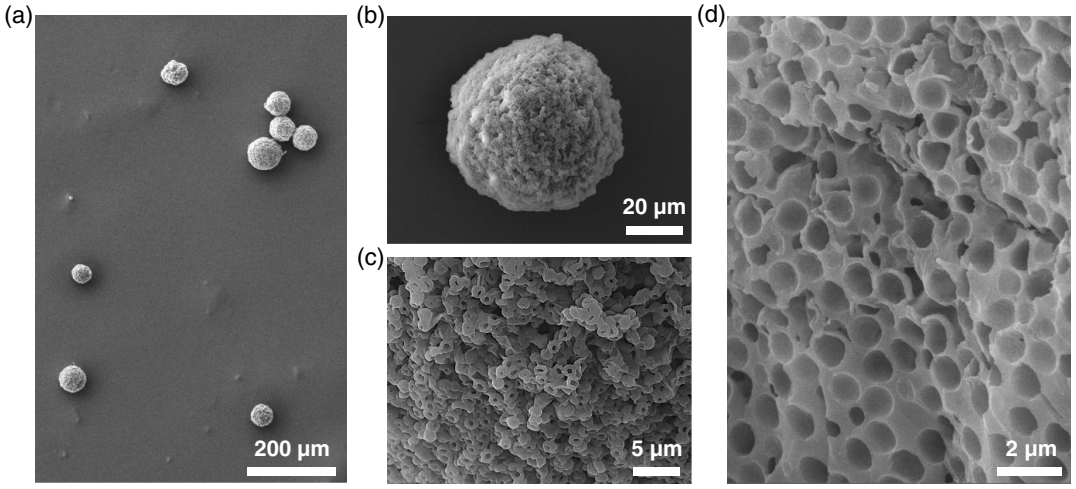

Figure 5. a) SEM image of fabricated microporous spheres with various diameters ranging from about 10 to 120 μm. b,c) SEM image of a single microporous sphere with a diameter of 80 μm and its porous surface, respectively. d) High-magnification SEM image of the microporous structure highlighting the air voids and the BSA structure.

© 2021 The Authors. Advanced Photonics Research published by Wiley-VCH GmbH

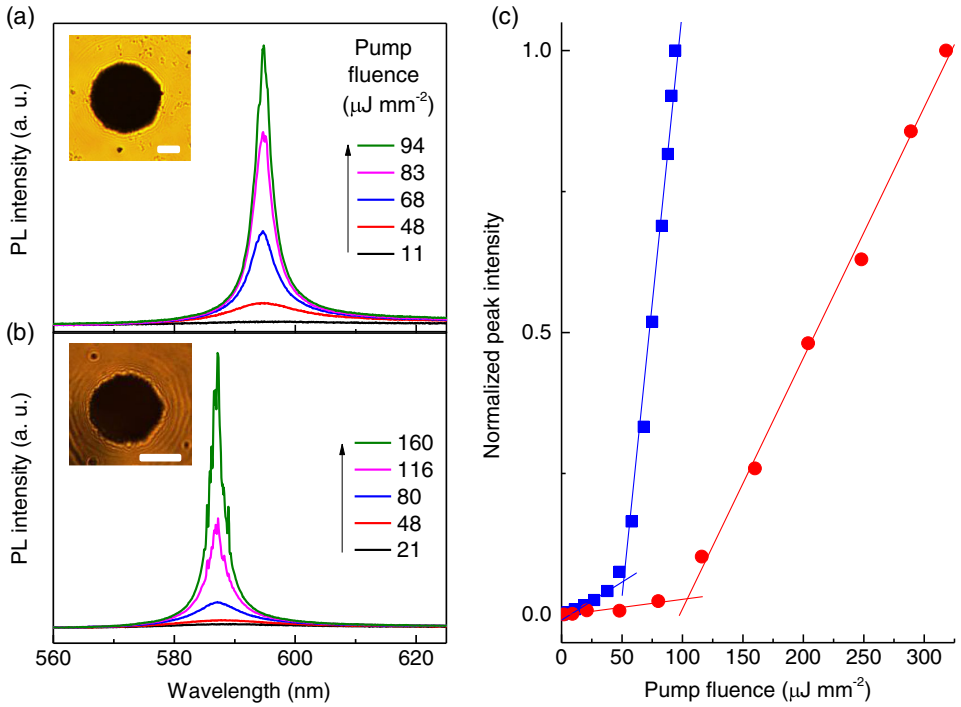

Figure 6. a) Emission spectra of a 70 μm diameter and b) a 35 μm diameter microporous protein sphere under various pump fluences. The scale bars are 20 μm. c) Normalized peak intensity of the emission of the two spheres 70 μm diameter (blue square), 35 μm diameter (red circular) as a function of pump fluence.

diameters as shown in Figure S4, Supporting Information. As a result, it is suggested that the lasing properties are mainly due to pore size and microsphere size and is not as much affected by the small differences in morphology/porosity.

5. Conclusion

We have demonstrated two kinds of novel organic random microlasers with size from 30 to 160 μm. These tiny random laser sources are in the form of microporous spheres with monodisperse pores of 1.28 μm made of dye-doped PVA or BSA. The lasing threshold is around 154 μJ mm^{-2} for a 75 μm diameter PVA sphere. Size dependence of lasing characteristics is investigated, and the result shows that the lasing spectrum, lasing wavelength, and lasing threshold are different between spheres. A smaller sphere exhibits a narrower spectrum compared with a larger one. The lasing wavelength is redshift with increase sphere diameter and a wavelength shift of 10 nm is obtained when the PVA-based laser diameter increases from 34 to 165 μm. The wavelength shift mechanism is ascribed to the reabsorption of light by the dye molecules. Furthermore, a smaller sphere exhibits a higher lasing threshold compared with a larger one. In particular, the lasing threshold is around 51 μJ mm^{-2} for a 70 μm diameter BSA sphere and it increases to 104 μJ mm^{-2} for a 35 μm diameter sphere. Our work provides a unique fabrication technique and structures for the realization of random microlasers which is significant for the fundamental study of light–matter interaction in a complex medium and promising applications in photonic integrated circuits, photonic barcode, optical sensing, and biointegration.

6. Experimental Section

Fabrication of Microporous PVA Spheres: The mixture used for the fabrication of microporous PVA spheres was prepared by subsequently mixing 1 mL aqueous PVA solution, 4 wt% and 0.4 mL aqueous suspension monodispersion PS microparticles, 10 wt%. To make random lasers, 0.1 mL aqueous RhB solution, 1 wt% serving as gain material was added. In addition, the 4 wt% PVA solution was obtained by magnetic stirring 0.8 g PVA powder ($M_w = 89\,000$–$98\,000$, from Sigma-Aldrich) in 20 mL deionized water at 80 °C for 4 h. The monodispersion PS microparticles were purchased from Particles GmbH. The microparticles had nearly the same diameter of 1.28 μm with a standard deviation of only 0.04 μm. From the aforementioned mixture, microporous PVA spheres were obtained using the fabrication process shown in Figure 1. The heating temperature was 100 °C for 90 min. The etching time was 30 h at room temperature.

Fabrication of Microporous BSA Spheres: The mixture used for the fabrication of microporous spheres was prepared by subsequently mixing 80 μL aqueous BSA solution, 10 wt% and 20 μL RhB aqueous solution, 2 wt% and 80 μL suspension PS microparticles, 10 wt%. From this mixture, RhB-doped microporous BSA spheres were fabricated by using the fabrication process shown in Figure 1. The heating temperature was 80 °C for 120 min. The etching time was 24 h at 70 °C. It was noted that the PS particles were hard to remove when etching at room temperature.

Optical Measurement: Individual microporous spheres were investigated by using a micro- PL (μ-PL) setup. The pumping source was a pulsed microchip Nd:YAG laser (from Teem Photonics) with a wavelength of 532 nm and a pulse duration of 400 ps. The pumping laser beam was guided and directed through an objective lens, magnification of either 10× or 20× of a Nikon Eclipse Ti-U inverted microscope, and collimated to a beam spot of ≈165 μm (for the 10×) or ≈80 μm (for the 20×) in diameter to excite the spheres. The pump energy was precisely controlled by an acousto-optic modulator. Emission from the spheres was collected through the same objective and coupled to a spectrometer for spectral recording. All optical measurements were conducted at room temperature and ambient conditions. It was noted that fabricated microporous spheres

© 2021 The Authors. Advanced Photonics Research published by Wiley-VCH GmbH

were generally stored in ethyl acetate to reduce the oxidation of the dye molecules. They were removed from the solvent and left to completely dry before optical characterization.

Supporting Information

Supporting Information is available from the Wiley Online Library or from the author.

Acknowledgements

This research was funded by Vietnam National Foundation for Science and Technology Development (NAFOSTED) under grant number 103.03-2017.318 and the the EPSRC Standard Grant EP/T027258. The authors thank Dr. Nghiem Thi Ha Lien for the assistance in measuring the absorption and emission of RhB aqueous solution.

Conflict of Interest

The authors declare no conflict of interest.

Data Availability Statement

Data underlying the results presented in this paper are available in Dataset, Ref. [37].

Keywords

bovine serum albumin, inverse photonic glass structures, microlasers, polyvinyl alcohol, random lasing

Received: February 9, 2021
Revised: March 30, 2021
Published online: June 25, 2021

[1] F. Luan, B. Gu, A. S. L. Gomes, K.-T. Yong, S. Wen, P. N. Prasad, *Nano Today* **2015**, *10*, 168.
[2] D. Wiersma, *Nature* **2000**, *406*, 132.
[3] N. M. Lawandy, R. M. Balachandran, A. S. L. Gomes, E. Sauvain, *Nature* **1994**, *368*, 436.
[4] Y. Chen, J. Herrnsdorf, B. Guilhabert, Y. Zhang, I. M. Watson, E. Gu, N. Laurand, M. D. Dawson, *Opt. Express* **2011**, *19*, 2996.
[5] Y. Wang, V. D. Ta, Y. Gao, T. C. He, R. Chen, E. Mutlugun, H. V. Demir, H. D. Sun, *Adv. Mater.* **2014**, *26*, 2954.
[6] H. Cao, Y. G. Zhao, S. T. Ho, E. W. Seelig, Q. H. Wang, R. P. H. Chang, *Phys. Rev. Lett.* **1999**, *82*, 2278.
[7] S. Gottardo, R. Sapienza, P. D. García, A. Blanco, D. S. Wiersma, C. López, *Nat. Photonics* **2008**, *2*, 429.
[8] Y. Chen, J. Herrnsdorf, B. Guilhabert, Y. Zhang, A. L. Kanibolotsky, P. J. Skabara, E. Gu, N. Laurand, M. D. Dawson, *Org. Electron.* **2012**, *13*, 1129.
[9] L. Cerdán, A. Costela, E. Enciso, I. García-Moreno, *Adv. Funct. Mater.* **2013**, *23*, 3916.
[10] V. D. Ta, T. T. Nguyen, T. H. L. Nghiem, H. N. Tran, A. T. Le, N. T. Dao, P. D. Duong, H. H. Mai, *Opt. Commun.* **2020**, *475*, 126207.
[11] R. Chen, Q. Ye, T. He, V. D. Ta, Y. Ying, Y.-Y. Tay, T. Wu, H. Sun, *Nano Lett.* **2013**, *13*, 734.
[12] R. C. Polson, Z. V. Vardeny, *Appl. Phys. Lett.* **2004**, *85*, 1289.
[13] M. T. Hill, M. C. Gather, *Nat. Photonics* **2014**, *8*, 908.
[14] H. Cao, J. Y. Xu, E. W. Seelig, R. P. H. Chang, *Appl. Phys. Lett.* **2000**, *76*, 2997.
[15] Y. Wu, Y. Ren, A. Chen, Z. Chen, Y. Liang, J. Li, G. Lou, H. Zhu, X. Gui, S. Wang, Z. Tang, *Nanoscale* **2017**, *9*, 6959.
[16] S. Caixeiro, M. Gaio, B. Marelli, F. G. Omenetto, R. Sapienza, *Adv. Opt. Mater.* **2016**, *4*, 998.
[17] A. Tulek, R. C. Polson, Z. V. Vardeny, *Nat. Phys.* **2010**, *6*, 303.
[18] M. Umar, K. Min, S. Kim, S. Kim, *Sci. Rep.* **2019**, *9*, 16266.
[19] J. Clark, G. Lanzani, *Nat. Photonics* **2010**, *4*, 438.
[20] V. D. Ta, Y. Wang, H. Sun, *Adv. Opt. Mater.* **2019**, *7*, 1900057.
[21] V. D. Ta, D. Saxena, S. Caixeiro, R. Sapienza, *Nanoscale* **2020**, *12*, 12357.
[22] W. Zhang, J. Yao, Y. S. Zhao, *Acc. Chem. Res.* **2016**, *49*, 1691.
[23] S. Caixeiro, M. Peruzzo, O. D. Onelli, S. Vignolini, R. Sapienza, *ACS Appl. Mater. Interfaces* **2017**, *9*, 7885.
[24] R. Sapienza, *Nat. Rev. Phys.* **2019**, *1*, 690.
[25] C. C. DeMerlis, D. R. Schoneker, *Food Chem. Toxicol.* **2003**, *41*, 319.
[26] N. Garcia, A. Z. Genack, A. A. Lisyansky, *Phys. Rev. B* **1992**, *46*, 14475.
[27] R. Sapienza, P. D. García, J. Bertolotti, M. D. Martín, Á. Blanco, L. Viña, C. López, D. S. Wiersma, *Phys. Rev. Lett.* **2007**, *99*, 233902.
[28] W.-J. Lin, Y.-M. Liao, H.-Y. Lin, G. Haider, S.-Y. Lin, W.-C. Liao, R.-T. Wei, P. Perumal, T.-Y. Chang, C.-Y. Tseng, Y.-S. Lo, H.-M. Lin, T.-W. Shih, J.-S. Hwang, T.-Y. Lin, Y.-F. Chen, *Org. Electron.* **2018**, *62*, 209.
[29] J. Fallert, R. J. B. Dietz, J. Sartor, D. Schneider, C. Klingshirn, H. Kalt, *Nat. Photon.* **2009**, *3*, 279.
[30] H. E. Türeci, L. Ge, S. Rotter, A. D. Stone, *Science* **2008**, *320*, 643.
[31] V. D. Ta, S. Yang, Y. Wang, Y. Gao, T. He, R. Chen, H. V. Demir, H. Sun, *Appl. Phys. Lett.* **2015**, *107*, 221103.
[32] C. Zhang, C.-L. Zou, Y. Zhao, C.-H. Dong, C. Wei, H. Wang, Y. Liu, G.-C. Guo, J. Yao, Y. S. Zhao, *Sci. Adv.* **2015**, *1*, e1500257.
[33] X. Ma, X. Sun, D. Hargrove, J. Chen, D. Song, Q. Dong, X. Lu, T.-H. Fan, Y. Fu, Y. Lei, *Sci. Rep.* **2016**, *6*, 19370.
[34] V. D. Ta, S. Caixeiro, F. M. Fernandes, R. Sapienza, *Adv. Opt. Mater.* **2017**, *5*, 1601022.
[35] T. V. Nguyen, N. V. Pham, H. H. Mai, D. C. Duong, H. H. Le, R. Sapienza, V.-D. Ta, *Soft Matter* **2019**, *15*, 9721.
[36] Y. Ling, H. Cao, A. L. Burin, M. A. Ratner, X. Liu, R. P. H. Chang, *Phys. Rev. A* **2001**, *64*, 063808.
[37] D. Ta, S. Caixeiro, D. Saxena, R. Sapienza, figshare, **2021**, https://doi.org/10.6084/m9.figshare.14447499.v1.

© 2021 The Authors. Advanced Photonics Research published by Wiley-VCH GmbH